

A Numerical Conformal Mapping Method for Harmonic Mixed Boundary Value Problems

A. Karageorghis,¹ N. S. Stylianopoulos,¹ and H. A. Zachariades¹

Received June 30, 1995

We describe a simple and versatile technique for the numerical solution of harmonic mixed boundary value problems in simply-connected domains. This technique is based on the theory of Riemann–Hilbert problems, and involves only the use of already existing conformal mapping and quadrature routines.

KEY WORDS: Conformal mapping; harmonic functions; boundary value problems.

1. INTRODUCTION

The aim of this paper is to describe a numerical procedure for the solution of plane harmonic mixed boundary value problems in simply-connected domains, including problems involving serious boundary singularities. This procedure is based on a formulation that emerges from the theory of Riemann–Hilbert problems [Henrici (1993); Muskhelishvili (1992); and Wen (1991)], and involves the following two main steps:

- Mapping conformally the original domain of definition of the problem onto the upper half plane. This is done by using one of the available numerical conformal mapping packages such as SCPACK [Trefethen (1989)], CONFPACK [Hough (1990)] or BKMPACK [Warby (1992)].
- Determining the unknown harmonic function (in fact, the full complex potential) by solving the transplanted harmonic problem in the upper half-plane. This requires the evaluation of Cauchy integrals along the real axis, and is performed using standard quadrature routines such as those given in the NAG Library.

¹ Department of Mathematics and Statistics, University of Cyprus, P.O. Box 537, Nicosia, Cyprus.

The central idea on which this technique is based is not new; similar procedures have been presented in the past, for example in Haas and Brauchli (1991); and Homentcovschi *et al.* (1978). However, in contrast to the objectives of these earlier papers, our main purpose here is to show how existing software for conformal mapping and quadrature may be used to devise a numerical scheme which: a) is very easy to implement, b) has a wide range of applicability and, c) can lead to solutions of very high accuracy.

2. THE GENERAL PROBLEM AND METHOD

2.1. Prescription

Let Ω be a simply-connected domain in the complex z -plane ($z = x + iy$) and let $a_1, b_1, a_2, b_2, \dots, a_n, b_n$ be $2n$ points, in counter-clockwise order, on its boundary $\partial\Omega$. Also, let

$$\begin{aligned} \partial\Omega_1 &= \widehat{a_1 b_1} \cup \widehat{a_2 b_2} \cup \dots \cup \widehat{a_n b_n} \\ \partial\Omega_2 &= \widehat{b_1 a_2} \cup \widehat{b_2 a_3} \cup \dots \cup \widehat{b_{n-1} a_n} \cup \widehat{b_n a_1} \end{aligned}$$

and consider the following boundary value problem

$$\nabla^2 \psi = 0 \quad \text{in } \Omega \tag{2.1}$$

$$\psi = \psi_1 \text{ on } \partial\Omega_1 \quad \text{and} \quad \frac{\partial \psi}{\partial n} = \psi_2 \text{ on } \partial\Omega_2 \tag{2.2}$$

where ψ_1 and ψ_2 are given functions and $\partial/\partial n$ denotes the outward normal derivative with respect to $\partial\Omega$.

We recall the following results in connection with the problem in Eqs. (2.1) and (2.2):

The harmonic conjugate ϕ of ψ satisfies the boundary value problem

$$\nabla^2 \phi = 0 \quad \text{in } \Omega \tag{2.3}$$

$$\frac{\partial \phi}{\partial n} = \frac{\partial \psi_1}{\partial s} \text{ on } \partial\Omega_1 \quad \text{and} \quad \frac{\partial \phi}{\partial s} = -\psi_2 \text{ on } \partial\Omega_2 \tag{2.4}$$

where $\partial/\partial s$ denotes the tangential derivative with respect to $\partial\Omega$. Here, the second of the boundary conditions in Eq. (2.4) can be written as

$$\begin{aligned} \phi &= \phi_2 + c_j && \text{on } \widehat{b_j a_{j+1}}, \quad j = 1, 2, \dots, n-1 \\ \phi &= \phi_2 + c_n && \text{on } \widehat{b_n a_1} \end{aligned}$$

where ϕ_2 is an antiderivative of $-\psi_2$ and c_1, c_2, \dots, c_n are real constants of integration.

Let T be a conformal mapping taking Ω onto the upper half plane $\text{Im } Z > 0$ ($Z = X + iY$), let $A_1, B_1, A_2, B_2, \dots, A_n, B_n$ be respectively the images of the points $a_1, b_1, a_2, b_2, \dots, a_n, b_n$ on the real axis, and let R_1 and R_2 denote the following two unions of real intervals,

$$R_1 = (A_1, B_1) \cup (A_2, B_2) \cup \dots \cup (A_n, B_n)$$

and

$$R_2 = (B_1, A_2) \cup \dots \cup (B_{n-1}, A_n) \cup (B_n, A_1)$$

Also, let

$$\Psi = \psi \circ T^{[-1]}, \quad \Phi = \phi \circ T^{[-1]}$$

Then, the transplanted potentials Ψ and Φ satisfy the following two mixed boundary value problems

$$\nabla^2 \Psi = 0 \quad \text{in } \text{Im } Z > 0 \tag{2.5}$$

$$\Psi = \Psi_1 \text{ on } R_1 \quad \text{and} \quad \frac{\partial \Psi}{\partial Y} = \frac{-\Psi_2}{|T'|} \text{ on } R_2 \tag{2.6}$$

and

$$\nabla^2 \Phi = 0 \quad \text{in } \text{Im } Z > 0 \tag{2.7}$$

$$\frac{\partial \Phi}{\partial Y} = \frac{-\partial \Psi_1}{\partial X} \quad \text{on } R_1 \tag{2.8}$$

and

$$\begin{aligned} \Phi &= \Phi_2 + c_j & \text{on } (B_j, A_{j+1}), \quad j = 1, 2, \dots, n-1 \\ \Phi &= \Phi_2 + c_n & \text{on } (B_n, A_1) \end{aligned} \tag{2.9}$$

where

$$\Psi_1 = \psi_1 \circ T^{[-1]}, \quad \Psi_2 = \psi_2 \circ T^{[-1]}, \quad \Phi_2 = \phi_2 \circ T^{[-1]} \tag{2.10}$$

It follows from this that the complex potential function $F(Z) = \Phi(X, Y) + i\Psi(X, Y)$ can be written as

$$F(Z) = i \frac{\sqrt{P(Z)}}{\pi} \int_{-\infty}^{\infty} \frac{\mu(t) dt}{\sqrt{P(t)}(Z-t)} \tag{2.11}$$

where

$$P(Z) = \prod_{j=1}^n (Z - A_j)(Z - B_j) \tag{2.12}$$

$$\mu(t) = \begin{cases} i\Psi_1(t) & \text{for } t \in R_1, \\ \Phi_2(t) + c_j & \text{for } t \in (B_j, A_{j+1}), j = 1, 2, \dots, n-1 \\ \Phi_2(t) + c_n & \text{for } t \in (-\infty, A_1) \cup (B_n, \infty) \end{cases} \tag{2.13}$$

and

$$\sqrt{P(t)} = \begin{cases} (-1)^n \sqrt{|P(t)|} & \text{for } t \in (-\infty, A_1), \\ (-1)^{n-j} i \sqrt{|P(t)|} & \text{for } t \in (A_j, B_j), j = 1, 2, \dots, n, \\ (-1)^{n-j} \sqrt{|P(t)|} & \text{for } t \in (B_j, A_{j+1}), j = 1, 2, \dots, n-1, \\ \sqrt{|P(t)|} & \text{for } t \in (B_n, \infty) \end{cases} \tag{2.14}$$

[see e.g., Homentcovschi (1980)]. For $F(Z)$ to be finite at $Z = \infty$ we impose the $n - 1$ conditions [Homentcovschi (1980); Wen (1991)]

$$\int_{-\infty}^{\infty} \frac{\mu(t) t^m}{\sqrt{P(t)}} dt = 0, \quad m = 0, 1, \dots, n-2 \tag{2.15}$$

which provide $n - 1$ equations for the determination of the constants c_j , $j = 1, 2, \dots, n$. This leaves one undetermined constant, and implies that the required complex potential is arbitrary to within a real constant. This arbitrariness can be eliminated by specifying the value of ϕ at one point on $\partial\Omega_2$.

Having found the constant coefficient c_j we express Eq. (2.11) as

$$F(Z) = i \frac{\sqrt{P(Z)}}{\pi} \left[\sum_{j=1}^n \int_{A_j}^{B_j} \frac{\mu(t) dt}{\sqrt{P(t)} (Z-t)} + \sum_{j=1}^{n-1} \int_{B_j}^{A_{j+1}} \frac{\mu(t) dt}{\sqrt{P(t)} (Z-t)} + \int_{B_n}^{\infty} \frac{\mu(t) dt}{\sqrt{P(t)} (Z-t)} + \int_{-\infty}^{A_1} \frac{\mu(t) dt}{\sqrt{P(t)} (Z-t)} \right] \tag{2.16}$$

The process for obtaining the solution of Eqs. (2.1) and (2.2), or indeed the full complex potential $f(z) = \phi(x, y) + i\psi(x, y)$, at a point (x_0, y_0) on $\Omega \cup \partial\Omega$ involves the following steps:

Step 1. Specify ϕ at one point on $\partial\Omega_2$ and solve the linear system resulting from Eqs. (2.15) for the constants c_j , $j = 1, \dots, n - 1$.

Step 2. Find the image $Z_0 = X_0 + iY_0$ of the point $z_0 = x_0 + iy_0$ under the mapping T .

Step 3. Compute $F(Z_0)$ using Eq. (2.16), and hence determine $f(z_0)$, $\phi(x_0, y_0)$ and $\psi(x_0, y_0)$ from

$$\begin{aligned} f(z_0) &= \phi(x_0, y_0) + i\psi(x_0, y_0) \\ &= F(Z_0) \end{aligned}$$

2.2. Implementational Considerations

(i) **Conformal mapping:** When the domain Ω of the problem is polygonal, we determine the conformal map T using the Schwarz–Christoffel numerical conformal package SCPACK [Trefethen (1989)]. This package is available in double precision, is highly accurate and easy to use.

If $\partial\Omega$ contains curved segments, we determine T via the numerical conformal mapping package CONFPACK [Hough (1990)], which is based on the integral equation formulation of Symm (1966). This package is only available in single precision. Alternatively, for domains with curved boundaries the numerical conformal mapping package BKMPACK [Warby (1992)] can be used. This is based on the Bergman kernel method of [Levin *et al.*, (1978)] and is available in double precision. Unfortunately, however, this package does not provide for the determination of the inverse map T^{-1} , which is needed for dealing with problems that involve nonconstant boundary conditions.

We note that each of the conformal mapping packages SCPACK, CONFPACK and BKMPACK is for mapping onto the unit disc. Thus, in order to obtain T we need to perform an additional bilinear transformation from the unit disc onto the upper half-plane.

(ii) **Quadrature:** The definite integrals appearing in Eq. (2.15) have integrands which are singular at the endpoints of the intervals of integration. If one endpoint is α , then the integrand singularity is of the form $|x - \alpha|^{-1/2}$. In order to evaluate these integrals we use the NAG routine D01APF. This is an adaptive integration routine for determining integrals of the form $\int_{\alpha}^{\beta} g(x) k(x) dx$, where $k(x) = (x - \alpha)^{s_1} (\beta - x)^{s_2}$, $s_1, s_2 > -1$, and $g(x)$ is well-behaved on $[\alpha, \beta]$. In it, the interval is repeatedly bisected and a modified Clenshaw–Curtis integration scheme is then used on all subintervals which include the endpoints. Gauss–Kronrod integration is applied to the remaining subintervals [Piessens *et al.* (1983)].

For the computation of the complex potential $F(Z)$, if Z is not on the real axis, then the integrands in Eq. (2.16) have the same singularities as before and are therefore computed by using again the NAG routine

D01APF. If, however, Z is a boundary point, then the integrand of one of the integrals in Eq. (2.16) has a singularity of the form $|x - \gamma|^{-1}$ where γ is a point in the interior of one of the intervals of integration. In this case the interval in question is subdivided into three subintervals, so that the middle one contains the singular point γ . The integrations on the first and third subintervals are carried out in exactly the same way as before (since there is an endpoint singularity of order $-\frac{1}{2}$ in each), while the middle integral is evaluated using the NAG routine D01AQF. This adaptive integration routine calculates an approximation to integrals of the form

$$\int_{\alpha}^{\beta} \left[\frac{g(x)}{x - \gamma} \right] dx, \quad \alpha < \gamma < \beta$$

in the Cauchy principal value sense. The strategy followed in this routine is almost identical to the one in D01APF [Piessens *et al.* (1983)].

The integrals over the semi-infinite intervals appearing in Eq. (2.16) may be evaluated with the NAG subroutine D01AMF. In this adaptive subroutine the semi-infinite intervals are first transformed onto finite ones via algebraic mappings and then evaluated over these by means of a process based on Gaussian and Kronrod integration.

3. NUMERICAL EXAMPLES

Example 3.1. Let Ω be the rectangle $\Omega = \{(x, y) : |x| < 7, 0 < y < 7\}$ and consider the boundary value problem (see Fig. 1).

$$\begin{aligned} \nabla^2 \psi &= 0 && \text{in } \Omega \\ \psi &= 500 && \text{on } a_1 b_1 \\ \frac{\partial \psi}{\partial y} &= 0 && \text{on } b_1 a_2 \\ \psi &= 1000 && \text{on } a_2 b_2 \\ \frac{\partial \psi}{\partial y} &= 0 && \text{on } b_2 d \\ \frac{\partial \psi}{\partial x} &= 0 && \text{on } da_1 \end{aligned}$$

This example, which is known as the Motz problem, has become a standard test for the performance of numerical methods for problems with

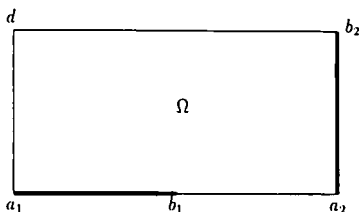


Fig. 1. The thick lines denote segments with Dirichlet conditions and the thin lines denote segments with Neumann conditions. The coordinates are given by $a_1(-7, 0)$, $b_1(0, 0)$, $a_2(7, 0)$, $b_2(7, 7)$ and $d(-7, 7)$.

boundary singularities. In this case the conformal map T is known exactly in terms of a Jacobian elliptic sine. Because of this, the exact solution of the problem may be found, in terms of elliptic integrals, by a conformal mapping method (Papamichael (1989), see [pp. 76, 77]; Rosser and Papamichael (1974); and Whiteman and Papamichael (1972)). In fact, if the exact T is used, then our scheme will lead to the exact solution given by Whiteman and Papamichael (1972) (see the remark in Homentcovschi (1980), [p. 361]). Here, however, in order to illustrate the application of our scheme, we perform T numerically using SCPACK and determine an approximation to ψ by quadrature as follows:

Since $\partial\psi/\partial n$ vanishes on each of the boundary segments b_1a_2 and b_2da_1 , the conjugate harmonic function ϕ takes constant values on each of these two segments. We are therefore free to specify one of these two constant values. Here we take

$$\phi = 0 \quad \text{on } b_2da_1 \tag{3.1}$$

If we let $\phi = c_1$ on b_1a_2 , then Eq. (2.15) with $n = 2$, gives

$$500i \int_{A_1}^{B_1} \frac{dt}{\sqrt{P(t)}} + c_1 \int_{B_1}^{A_2} \frac{dt}{\sqrt{P(t)}} + 1000 \int_{A_2}^{B_2} \frac{dt}{\sqrt{B(t)}} = 0 \tag{3.2}$$

(because of Eq. (3.1), the integrals over the intervals $(-\infty, A_1)$ and (B_2, ∞) do not appear in Eq. (3.2)). Hence, by using the NAG routine D01APF for the computation of the three integrals in Eq. (3.2), we find the following approximation to c_1 ,

$$\tilde{c}_1 = 340.317086529956$$

Finally, an approximation to the full complex potential $F(Z)$ can be determined from Eq. (2.16), i.e., from

$$F(Z) = \frac{\sqrt{P(Z)}}{\pi} \left[500 \int_{A_1}^{B_1} \frac{dt}{\sqrt{P(t)}(Z-t)} - ic_1 \int_{B_1}^{A_2} \frac{dt}{\sqrt{P(t)}(Z-t)} + 1000 \int_{A_2}^{B_2} \frac{dt}{\sqrt{P(t)}(Z-t)} \right] \quad (3.3)$$

as indicated in Section 2.2(ii), by computing the integrals using the NAG routines D01APF and D01AQF.

We used this process to compute approximations to the harmonic function $\psi = \text{Im}\{F \circ T^{-1}\}$ on a square grid of size 0.1 covering $\Omega \cup \partial\Omega$. We then compared these approximations to the corresponding exact values obtained from the series solution given by Rosser and Papamichael (1974). The absolute error was uniform throughout the grid and of order 10^{-13} . For example at the point (0.1, 0.1) the numerical process gave the approximation

$$\tilde{\psi} = 552.775750977129$$

which agrees with the exact solution there to all given figures. We note that the SCPACK estimate of the error in the corresponding approximation to the conformal map onto the unit disc was, in this case, 4.65×10^{-15} . In order to test the performance of the algorithm when integrals over semi-infinite domains are involved we also solved the problem when choosing

$$\phi = 0 \quad \text{on } b_1 a_2 \quad (3.4)$$

instead of Eq. (3.1). As a consequence of this, semi-infinite integrals appear in the equations corresponding to Eqs (3.2) and (3.3). The results were identical to the ones obtained when choosing the condition of Eq. (3.1).

Example 3.2. Let Ω be the L -shaped domain

$$\Omega = \{(x, y): 0 < x < 2, 0 < y < 1\} \cup \{(x, y): 0 < x < 1, 0 < y < 2\}$$

illustrated in Fig. 2. and consider the boundary value problem

$$\begin{aligned} \nabla^2 \psi &= 0 && \text{in } \Omega \\ \psi &= 0 && \text{on } a_1 b_1 \\ \psi &= 1 && \text{on } a_2 b_2 \\ \psi &= 2 && \text{on } a_3 b_3 \\ \frac{\partial \psi}{\partial n} &= 0 && \text{on } b_1 a_2, b_2 a_3, b_3 a_1 \end{aligned}$$

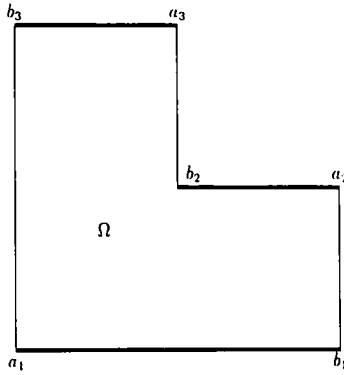


Fig. 2. The boundary of the region of integration is divided into six segments. Segments drawn with thick lines have Dirichlet conditions. The coordinates of the points are $a_1(0, 0)$, $b_1(2, 0)$, $a_2(2, 1)$, $b_2(1, 1)$, $a_3(1, 2)$ and $b_3(0, 2)$.

The exact solution of this problem is $\psi = y$. The conformal mapping T was performed numerically using SCPACK.

Equations (2.15) with $n = 3$ provide two equations for the constants c_1, c_2, c_3 where $\phi = c_1$ on (B_1, A_2) , $\phi = c_2$ on (B_2, A_3) , and $\phi = c_3$ on $(B_3, \infty) \cup (-\infty, A_1)$. We choose $c_3 = 0$ and obtain c_1 and c_2 from

$$c_1 \int_{B_1}^{A_2} \frac{dt}{\sqrt{P(t)}} + i \int_{A_2}^{B_2} \frac{dt}{\sqrt{P(t)}} + c_2 \int_{B_2}^{A_3} \frac{dt}{\sqrt{P(t)}} + 2i \int_{A_3}^{B_3} \frac{dt}{\sqrt{P(t)}} = 0 \quad (3.5)$$

and

$$c_1 \int_{B_1}^{A_2} \frac{t dt}{\sqrt{P(t)}} + i \int_{A_2}^{B_2} \frac{t dt}{\sqrt{P(t)}} + c_2 \int_{B_2}^{A_3} \frac{t dt}{\sqrt{P(t)}} + 2i \int_{A_3}^{B_3} \frac{t dt}{\sqrt{P(t)}} = 0 \quad (3.6)$$

The approximate solution was evaluated on a square grid of size 0.2 covering $\Omega \cup \partial\Omega$. The absolute error was again uniform throughout the grid and of order 10^{-14} . The SCPACK error estimate was, in this case, 8.96×10^{-15} .

Example 3.3. Let Ω be the L-shaped domain of Example 3.2, and consider the boundary value problem

$$\begin{aligned} \nabla^2 \psi &= 0 && \text{in } \Omega \\ \psi &= x^2 && \text{on } a_1 b_1 \end{aligned}$$

$$\begin{aligned} \frac{\partial \psi}{\partial n} &= 4 && \text{on } b_1 a_2 \\ \psi &= x^2 - 1 && \text{on } a_2 b_2 \\ \frac{\partial \psi}{\partial n} &= 2 && \text{on } b_2 a_3 \\ \psi &= x^2 - 4 && \text{on } a_3 b_3 \\ \frac{\partial \psi}{\partial n} &= 0 && \text{on } b_3 a_1 \end{aligned}$$

The exact solution of this problem is $\psi = x^2 - y^2$. This problem has the added difficulty that the boundary conditions for ϕ are no longer constant. This means that the functions $\Phi_2(t)$ appearing in Eq. (2.13) are no longer constant and have to be determined from $\Phi_2 = \phi_2 \circ T^{[-1]}$ for each evaluation of the integrand. Equation (2.15) with $n=3$ provide two equations for the constants c_1, c_2, c_3 where $\phi = -4y + c_1$ on $b_1 a_2$, $\phi = -2y + c_2$ on $b_2 a_3$ and $\phi = c_3$ on $b_3 a_1$. We choose $c_3 = 0$ as in Example 3.2.

The approximate solution was evaluated on uniform square grid of size 0.2 as in Example 3.2. The absolute error was again found to be uniform throughout the grid and of order 10^{-12} . The lower order of accuracy in this problem occurs because of the presence of extra errors in the integrands due to the approximate evaluations of the inverse conformal mapping.

Example 3.4. Let Ω be the curved domain

$$\Omega = \{(x, y): x^2 + y^2 < 1, y > 0\} \cup \{(x, y): x^2 + y^2 < 1, x < 0\}$$

of Fig. 3, and consider the boundary value problem

$$\begin{aligned} \nabla^2 \psi &= 0 && \text{in } \Omega \\ \psi &= x && \text{on } a_1 b_1 \\ \frac{\partial \psi}{\partial n} &= x && \text{on } b_1 a_2 \\ \psi &= x && \text{on } a_2 b_2 \\ \frac{\partial \psi}{\partial n} &= 1 && \text{on } b_2 a_3 \\ \psi &= 0 && \text{on } a_3 b_3 \\ \frac{\partial \psi}{\partial n} &= 0 && \text{on } b_3 a_1 \end{aligned}$$

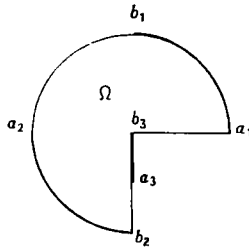


Fig. 3. A domain with a curved boundary. Segments drawn with thick lines indicate Dirichlet conditions. The coordinates of the points are $a_1(1, 0)$, $b_1(0, 1)$, $a_2(-1, 0)$, $b_2(0, -1)$, $a_3(0, -1/2)$ and $b_3(0, 0)$.

The exact solution is $\psi = x$. From Eq. (2.15) with $n=3$ we get two equations for the determination of c_1, c_2, c_3 where $\phi = -y + c_1$ on b_1a_2 , $\phi = -y + c_2$ on b_2a_3 and $\phi = c_3$ on b_3a_1 . We again choose $c_3 = 0$.

The presence of the curved boundary means that it is no longer possible to use SCPACK. Instead, the package CONFPACK was used. The errors were calculated on a 0.25×0.25 uniform grid in the domain of the problem. In this case the absolute error was found to be of order 10^{-4} , which is much larger than in the previous examples. This is due to the complexity of the domain and the fact that CONFPACK is a single precision package. The CONFPACK estimate for the approximation to the conformal map onto the unit disk was, in this case, 4.9×10^{-6} .

ACKNOWLEDGMENT

We wish to thank Professor N. Papamichael for many valuable suggestions.

REFERENCES

- Haas, R., and Brauchli, H. (1991). Fast solver for plane potential problems with mixed boundary conditions. *Comput. Methods Appl. Mech. Engng.* **89**, 543–556.
- Henrici, P. (1993). *Applied and Computational Complex Analysis*, Vol. III, J. Wiley, London.
- Homentcovschi, D. (1980). On the mixed boundary-value problem for harmonic functions in plane domains. *Z. Angew. Math. Phys.* **31**, 352–366.
- Homentcovschi, D., Manolescu, A., Manolescu, A. M., and Burileanu, C. (1978). A general approach to analysis of distributed resistive structures. *IEEE Trans. Electron Devices* **ED-25**, 7, 787–794.
- Hough, D. M. (1990). User's Guide to CONFPACK IPS, Research Report No. 90-11 ETH, Zürich.
- Levin, D., Papamichael, N., and Sideridis, A. (1978). The Bergman kernel method for the numerical conformal mapping of simply connected domains. *J. Inst. Math. Applies.* **22**, 171–187.

- Muskhelishvili, N. I. (1992). *Singular Integral Equations*, Dover Publications, New York.
- Numerical Algorithms Group Library Mark 15, 1991 NAG (UK) Ltd. Wilkinson House, Jordan Hill Road, Oxford, United Kingdom.
- Papamichael, N. (1989). Numerical conformal mapping onto a rectangle with applications to the solution of Laplacian problems. *J. Comput. Appl. Math.* **28**, 63–83.
- Piessens, R., de Doncker-Kapenga, E., Uberhuber, C. W., and Kahaner, D. K. (1983). *QUADPACK A Subroutine Package for Automatic Integration*, Springer-Verlag, Berlin.
- Rosser, J. B., and Papamichael, N. (1974). A power series solution for a harmonic mixed boundary value problem. MRC Techn. Summary Report No. 1405 University of Wisconsin-Madison.
- Symm, G. T. (1966). An integral equation method in conformal mapping. *Numer. Math.* **9**, 250–258.
- Trefethen, L. N. (1989). SCPACK User's Guide, Numerical Analysis Report 89-2, Department of Mathematics, MIT.
- Warby, M. K. (1992). BKMPACK User's Guide, Technical Report, Department of Mathematics and Statistics, Brunel University.
- Wen, G. C. (1991). *Conformal Mappings and Boundary Value Problems, Translation of Mathematical Monographs*, Vol. 106, American Mathematical Society, Providence, Rhode Island.
- Whiteman, J. R., and Papamichael, N. (1972). Treatment of harmonic mixed boundary value problems by conformal transformation methods. *Z. Angew. Math. Phys.* **23**, 655–664.